

Voids fill us in on rising cosmology tensions

Sofia Contarini ^{1,2,3} Alice Pisani ^{4,5,6} Nico Hamaus ⁷ Federico Marulli^{1,2,3} , Lauro Moscardini^{1,2,3} , and Marco Baldi^{1,2,3} 

¹Dipartimento di Fisica e Astronomia “Augusto Righi” - Alma Mater Studiorum Università di Bologna, via Piero Gobetti 93/2, I-40129 Bologna, Italy

²INFN-Sezione di Bologna, Viale Berti Pichat 6/2, I-40127 Bologna, Italy

³INAF-Osservatorio di Astrofisica e Scienza dello Spazio di Bologna, Via Piero Gobetti 93/3, I-40129 Bologna, Italy

⁴Center for Computational Astrophysics, Flatiron Institute, 162 5th Avenue, 10010, New York, NY, USA

⁵The Cooper Union for the Advancement of Science and Art, 41 Cooper Square, New York, NY 10003, USA

⁶Department of Astrophysical Sciences, Peyton Hall, Princeton University, 4 Ivy Lane, Princeton, NJ 08544, USA

⁷Universitäts-Sternwarte München, Fakultät für Physik, Ludwig-Maximilians-Universität, Scheinerstrasse 1, 81679 München, Germany

Abstract

We investigate the main tensions within the current standard model of cosmology from the perspective of the void size function in BOSS DR12 data. For this purpose, we present the first cosmological constraints on the parameters $S_8 \equiv \sigma_8 \sqrt{\Omega_m/0.3}$ and H_0 obtained from voids as a stand-alone probe. We rely on an extension of the popular volume-conserving model for the void size function, tailored to the application on data, including geometric and dynamic distortions. We calibrate the two nuisance parameters of this model with the official BOSS collaboration mock catalogs and propagate their uncertainty through the statistical analysis of the BOSS void number counts. We focus our analysis on the Ω_m - σ_8 and Ω_m - H_0 parameter planes and derive the marginalized constraints $S_8 = 0.78^{+0.16}_{-0.14}$ and $H_0 = 65.2^{+4.5}_{-3.6}$ km s⁻¹ Mpc⁻¹. Our estimate of S_8 is fully compatible with constraints from the literature, while our H_0 value slightly disagrees by more than 1σ with recent local distance ladder measurements of type Ia supernovae. Our results open up a new viewing angle on the rising cosmological tensions and are expected to improve notably in precision when jointly analyzed with independent probes.

Unified Astronomy Thesaurus concepts: cosmology: observations, cosmological parameters, large-scale structure of universe, methods: statistical

1. Introduction

In recent years, anomalies in the observations of the Universe at large scales have puzzled the scientific community. These are expressed as statistically relevant discrepancies, or tensions, between the cosmological constraints obtained from late (i.e. low-redshift) and early (i.e. high-redshift) probes.

The most significant tension affects the estimate of the Hubble constant, H_0 , describing the present expansion rate of the Universe. In particular, the so-called *Hubble tension* concerns the mismatch between the Planck collaboration results obtained from the cosmic microwave background (CMB) anisotropies (Planck Collaboration et al. 2020), and the direct local distance ladder measurements based on type Ia supernovae (SN Ia, Riess

et al. 2022). These two estimates are in disagreement by about 5σ (see, e.g., Di Valentino et al. 2021a). Second in order of importance is the tension on the matter clustering strength, often quantified by the parameter $S_8 \equiv \sigma_8 \sqrt{\Omega_m/0.3}$, derived from the matter density parameter Ω_m and the root mean square of density fluctuations on an $8 h^{-1}$ Mpc comoving scale, σ_8 . In this case the discrepancy of the Planck satellite measurements relates to low-redshift probes, like weak gravitational lensing and galaxy clustering, with a statistical disagreement at the level of 2 - 3σ (see, e.g., Di Valentino et al. 2021b).

These observational tensions may reveal the presence of systematic errors in the cosmological measurements or, alternatively, the requirement to modify the current benchmark Λ -cold dark matter (Λ CDM) model of cosmology. This has led to the proposal of a plethora of alternatives to the Λ CDM model, involving physics beyond the standard model of particle physics (see Abdalla

Corresponding author: Sofia Contarini
sofia.contarini3@unibo.it

et al. 2022, and references therein). Despite the fact that some of the proposed models alleviate one or more discrepancies (see, e.g., Pandey et al. 2020; Di Valentino et al. 2021c; Schöneberg et al. 2022), we are still longing for a definitive solution that provides a comprehensive and satisfactory description of all the cosmological observables.

In this context, the darkest regions of our Universe may supply a fundamental and independent contribution in shedding light on the rising cosmological tensions. These vast underdense zones, scarcely populated by galaxies and other luminous objects, are commonly referred to as *cosmic voids*. Within the last decade, voids have begun to assert their relevance as cosmological probes (Pisani et al. 2019; Moresco et al. 2022). Recent works have indeed exploited voids to test the standard cosmological model (e.g., Hamaus et al. 2016, 2020; Aubert et al. 2022; Nadathur et al. 2020; Woodfinden et al. 2022; Kovács et al. 2022) and others have provided promising forecasts on the constraining power expected from different void statistics with the upcoming redshift surveys, such as *Euclid* (Laureijs et al. 2011; Amendola et al. 2018; Hamaus et al. 2022; Contarini et al. 2022a; Bonici et al. 2022).

Nevertheless, up until now the void size function as a first-order statistic of voids has never been exploited to derive cosmological constraints. In this work we extend the results presented in Contarini et al. (2022b), where we performed a statistical analysis of the size distribution of voids identified in the final data release (DR12) of the Baryon Oscillation Spectroscopic Survey (BOSS, Eisenstein et al. 2011; Dawson et al. 2013). Here we make use of that same data to investigate the main cosmological tensions and provide a first estimate of the parameters S_8 and H_0 derived from cosmic voids. Finally, we discuss our results in the current context of cosmology, featuring the constraints from different surveys and cosmological probes.

This *Letter* is structured as follows. In Section 2 we present the theory of the void size function, together with the galaxy and void catalogs we employed. In Section 3 we describe the cosmological analysis performed in this work. The constraints obtained in this context are then presented in Section 4 and compared with other important results from the literature. Finally, in Section 5 we draw the conclusion of this work.

2. Theory and data sets

2.1. Void size function model

The void size function model predicts the comoving number density of voids as a function of their size. It was originally developed by Sheth & van de Weygaert

(2004) on the basis of the excursion-set theory and at its core relies on the multiplicity function:

$$f_{\ln \sigma_m}(\sigma_m) = 2 \sum_{j=1}^{\infty} \exp\left(-\frac{(j\pi x)^2}{2}\right) j\pi x^2 \sin(j\pi \mathcal{D}),$$

$$\text{with } \mathcal{D} = \frac{|\delta_v^L|}{\delta_c^L + |\delta_v^L|} \quad \text{and} \quad x = \frac{\mathcal{D}}{|\delta_v^L|} \sigma_m, \quad (1)$$

which describes the volume fraction of the Universe occupied by cosmic voids. In Equation (1) all the quantities are expressed in linear theory, as indicated by the superscript ‘‘L’’. In particular, σ_m is the root mean square variance of linear matter perturbations on a scale R_L , while δ_c^L and δ_v^L are the density contrasts required for the formation of dark matter halos and cosmic voids, respectively. Only the latter threshold significantly affects the predicted void size distribution at large scales and determines the linear density contrast embedded inside cosmic voids. We highlight the importance of this quantity further below, but refer the reader to Contarini et al. (2022b) for a more complete description.

To calculate the density of cosmic voids as a function of their radii R in the nonlinear regime, Jennings et al. (2013) proposed the following expression:

$$\frac{dn}{d \ln R} = \frac{f_{\ln \sigma_m}(\sigma_m)}{V(R)} \left. \frac{d \ln \sigma_m^{-1}}{d \ln R_L} \right|_{R_L=R_L(R)}, \quad (2)$$

which is called *volume-conserving model* (Vdn hereafter). As the name suggests, it relies on the conservation of the total volume V , occupied by voids in the transition from the linear to the nonlinear regime. The Vdn model has been tested successively in different works (see, e.g., Jennings et al. 2013; Ronconi et al. 2019; Verza et al. 2019; Contarini et al. 2021), but for its application to voids identified in a biased distribution of tracers (e.g., galaxies and clusters of galaxies) a modification of its main assumptions is required.

To take into account the change in the density contrast when voids are traced by biased objects, Contarini et al. (2019) introduced a simple parametrization of the underdensity threshold of the Vdn model. This strategy was then revisited in Contarini et al. (2022b) to take into account the degeneracy of the tracer effective bias with the normalization of the matter density fluctuations, σ_8 , leading to the following parametrization of the void density threshold:

$$\delta_{v,DM}^{NL} = \frac{\delta_{v,tr}^{NL}}{\mathcal{F}(b_{\text{eff}}, \sigma_8)}, \quad \text{with} \quad (3)$$

$$\mathcal{F}(b_{\text{eff}}, \sigma_8) = C_{\text{slope}} b_{\text{eff}} \sigma_8 + C_{\text{offset}}.$$

In this equation, we use the subscript ‘‘NL’’ to highlight quantities computed in nonlinear theory. Furthermore,

$\delta_{v, \text{tr}}^{\text{NL}}$ is the density contrast used to define voids in the tracer density field (tr), while $\delta_{v, \text{DM}}^{\text{NL}}$ is the corresponding value in the matter density field (DM, i.e. dark matter particles). The function $\mathcal{F}(b_{\text{eff}} \sigma_8)$ parametrizes the action of the tracer effective bias b_{eff} , which depends on redshift and on the selected tracers (e.g., their host-halo mass). C_{slope} and C_{offset} are redshift-independent coefficients of the linear function \mathcal{F} and their dependence on the cosmological model can be considered negligible (Contarini et al. 2021). Moreover, Contarini et al. (2022a) demonstrated that the parametrization presented in Equation (3) is effective in encapsulating redshift-space distortions on cosmic voids, i.e. the enlargement of their observed radii caused by the peculiar motions of their tracers.

The presented extension of the Vdn model predicts the size function of voids identified by biased tracers in redshift space with good accuracy, provided the calibration of the nuisance parameters of the model, C_{slope} and C_{offset} , is performed via mock catalogs designed to reproduce the target tracer population (see Contarini et al. 2021, for further details). Hereafter, we will refer to this theoretical framework as the *extended* Vdn model.

2.2. Galaxy and void catalogs

In this work we analyze the BOSS DR12 data set (Reid et al. 2016), composed of the two target selections LOWZ and CMASS featuring more than one million galaxies with spectroscopic redshifts. We further use 100 realizations of the MultiDark PATCHY mocks (Kitaura et al. 2014, 2016; Klypin et al. 2016; Rodríguez-Torres et al. 2016), specifically designed to mimic the properties of the BOSS galaxies, to calibrate the nuisance parameters of the extended Vdn model (see Section 2.1).

Following the procedure of Contarini et al. (2022b), we divide the catalogs into two redshift bins, i.e. $0.2 < z \leq 0.45$ and $0.45 < z < 0.65$, and measure $b_{\text{eff}} \sigma_8$ for each case, as required in Equation (3). We estimate this quantity by modeling the multipoles of the galaxy two-point correlation function with the prescriptions of Taruya et al. (2010) (see Appendix A of Contarini et al. 2022b for further details). For the BOSS galaxies this yields $b_{\text{eff}} \sigma_8 = 1.36 \pm 0.05$ in the interval $0.2 < z \leq 0.45$ and $b_{\text{eff}} \sigma_8 = 1.28 \pm 0.06$ in the $0.45 < z < 0.65$ interval.

To identify cosmic voids in the distribution of real and mock galaxies we apply the public Void IDentification and Examination toolkit¹ (VIDE, Sutter et al. 2015), based on the code ZOnes Bordering On Voidness (ZOBOV, Neyrinck 2008). VIDE exploits the Voronoi

tessellation technique to approximate a continuous density field and identifies its local minima. From this a catalog of voids is built by means of a watershed algorithm (Platen et al. 2007). We run VIDE on the entire galaxy distribution from the northern and southern Galactic hemispheres and assume the same cosmological model used to build the MultiDark PATCHY simulations to convert redshifts to comoving distances, i.e. a Planck2013 cosmology (Planck Collaboration et al. 2014, see also Section 3).

Once the voids are identified, we process the extracted sample to match the theoretical definition used in the void size function model. In particular, we apply the cleaning procedure developed by Ronconi & Marulli (2017), publicly available in the *free software* C++/Python libraries CosmoBolognaLib² (Marulli et al. 2016), which rescales voids such that they exhibit a fixed density contrast of $\delta_{v, \text{tr}}^{\text{NL}} = -0.7$. This choice of under-density threshold is not unique, but is especially suited to obtain a statistically reliable void sample (see, e.g., Contarini et al. 2022a, for further details).

We then measure number counts of the cleaned voids as a function of their size. In order to convert the predictions of the extended Vdn model from a void number density to number counts, we derive the effective survey volume calculated by VIDE via summation over all the Voronoi cells used to sample the tracer distribution (see Contarini et al. 2022b, for further details).

We first use the average PATCHY void number counts to calibrate the values of C_{slope} and C_{offset} through a Markov chain Monte Carlo (MCMC) analysis. The best-fit values we obtain for the coefficients of $\mathcal{F}(b_{\text{eff}} \sigma_8)$ are $C_{\text{slope}} = -1.62_{-0.73}^{+0.66}$ and $C_{\text{offset}} = 4.30_{-0.86}^{+0.94}$, but we refer the reader to Contarini et al. (2022b) for a complete presentation of these results. We then exploit the calibration performed with the PATCHY mocks to model the BOSS void number counts, sampling the posterior distribution of the free parameters of the extended Vdn model (see Section 3). We underline that the effectiveness of the analysis we apply in this work has been tested in Appendix B of Contarini et al. (2022b), where the methodology is thoroughly validated on PATCHY mocks.

3. Analysis

The cosmological analysis we carry out in this work is based on Bayesian inference. We take as data set the void counts extracted from the BOSS DR12 and assume a Poissonian likelihood (Sahlén et al. 2016). Our model is based on the extended Vdn theory, so it depends on

¹ https://bitbucket.org/cosmicvoids/vid_e_public

² <https://gitlab.com/federicomarulli/CosmoBolognaLib>

the cosmological model and on the nuisance parameters C_{slope} and C_{offset} (see [Section 2.1](#)).

We consider a flat Λ CDM model with fiducial parameters given by Planck2013 results ([Planck Collaboration et al. 2014](#)) to be consistent with the ones used to build the MultiDark PATCHY simulations: $\Omega_{\text{m}} = 0.307115$, $H_0 = 67.77 \text{ km s}^{-1} \text{ Mpc}^{-1}$, $\Omega_{\text{b}} = 0.048206$, $n_{\text{s}} = 0.9611$ and $\sigma_8 = 0.8288$. Our statistical analysis is aimed at investigating the degeneracies in the $\Omega_{\text{m}}-\sigma_8$ and $\Omega_{\text{m}}-H_0$ planes, so we focus on two sets of cosmological parameters, the first characterized by wide uniform priors for Ω_{m} and σ_8 , and the second for Ω_{m} and H_0 . In both cases we marginalize over the remaining cosmological parameters by assigning to them uniform priors centered on our fiducial cosmology and with a total width of ten times the 68% uncertainties provided by Planck2018 constraints ([Planck Collaboration et al. 2020](#)). We also marginalize over C_{slope} and C_{offset} by considering their joint posterior distribution obtained from the calibration with PATCHY mocks.

We finally sample the posterior distribution of the considered parameter sets following an MCMC technique. At each step of the MCMC we consider a new set of cosmological parameters, compute the void size function model and rescale the predicted void radii to take into account the effect of geometric distortions. The latter arise when assuming a wrong cosmology in the redshift-distance conversion, causing a distortion of the observed void shape along the directions parallel and perpendicular to the line of sight. The resulting anisotropy is referred to as Alcock-Paczynski (AP) effect ([Alcock & Paczynski 1979](#)) and can be modeled via two scaling parameters q_{\parallel} and q_{\perp} (e.g., [Sánchez et al. 2017](#)). Let us indicate with r_{\parallel}^* and r_{\perp}^* the observed comoving distances between two objects at redshift z , projected along the parallel and perpendicular line-of-sight directions, respectively. To obtain their corresponding length in the true cosmological model, we use:

$$\begin{aligned} r_{\parallel} &= \frac{H^*(z)}{H(z)} r_{\parallel}^* \equiv q_{\parallel} r_{\parallel}^*, \\ r_{\perp} &= \frac{D_{\text{A}}(z)}{D_{\text{A}}^*(z)} r_{\perp}^* \equiv q_{\perp} r_{\perp}^*. \end{aligned} \quad (4)$$

In these equations the starred quantities are computed assuming the fiducial cosmology. $H(z)$ is the Hubble parameter and $D_{\text{A}}(z)$ the comoving angular-diameter distance, which in flat Λ CDM are defined as:

$$\begin{aligned} H(z) &= H_0 [\Omega_{\text{m}}(1+z)^3 + 1 - \Omega_{\text{m}}]^{1/2} \quad \text{and} \\ D_{\text{A}}(z) &= \int_0^z \frac{c}{H(z')} dz', \end{aligned} \quad (5)$$

respectively. The inclusion of geometric distortions in the void size function model causes a shift in the predicted radius distribution that depends on the discrepancy between the true and the assumed fiducial cosmology. In [Section 4.1](#) we investigate the impact of this correction on the cosmological constraints. We finally underline that we did not account for super-sample covariance in our model, which recently has been demonstrated to only marginally affect the void size function ([Bayer et al. 2022](#)).

4. Results

4.1. Cosmological constraints from void counts

In this section we present the main results of the analysis, expressed as new cosmological constraints from the BOSS DR12 data set. These results supplement the constraints presented in [Contarini et al. \(2022b\)](#).

In [Figure 1](#) we show the results obtained when assuming a void size function model with Ω_{m} and σ_8 as free parameters (see [Section 3](#)). The marginalized cosmological constraints are $\Omega_{\text{m}} = 0.286_{-0.057}^{+0.070}$ and $\sigma_8 = 0.797_{-0.081}^{+0.094}$. In the left panels of [Figure 1](#) we show the associated confidence contours on the $\Omega_{\text{m}}-\sigma_8$ parameter plane. As a reference, we also report the constraints obtained when omitting the AP effect in our model (see [Section 3](#)). This allows us to quantify the improvement on our estimate of Ω_{m} and σ_8 due to the geometric distortion correction. We underline that this correction is generally negligible for collapsed and virialised structures, like galaxy clusters, because of their detachment from the Hubble expansion. This distinction is fundamental when constraining H_0 and represents an important advantage of the void size function with respect to the cluster mass function, for example.

In the right panels of [Figure 1](#) we compare our results with those obtained with other cosmological probes, focusing once again on the $\Omega_{\text{m}}-\sigma_8$ parameter plane. Besides the constraints presented in this work we report another result derived with cosmic voids, i.e. from the void-galaxy cross-correlation function in the BOSS DR12 data set. Utilizing voids as standard spheres to measure geometric distortions, [Hamaus et al. \(2020\)](#) constrained the growth rate of structure and provided a precise estimate of Ω_{m} , here reported as a continuous band. In the same plot we report the confidence contours computed by [Lesci et al. \(2022\)](#) with the mass function of clusters identified in the third data release of the Kilo Degree Survey (KiDS-DR3) and those of the combined analysis of galaxy clustering and weak gravi-

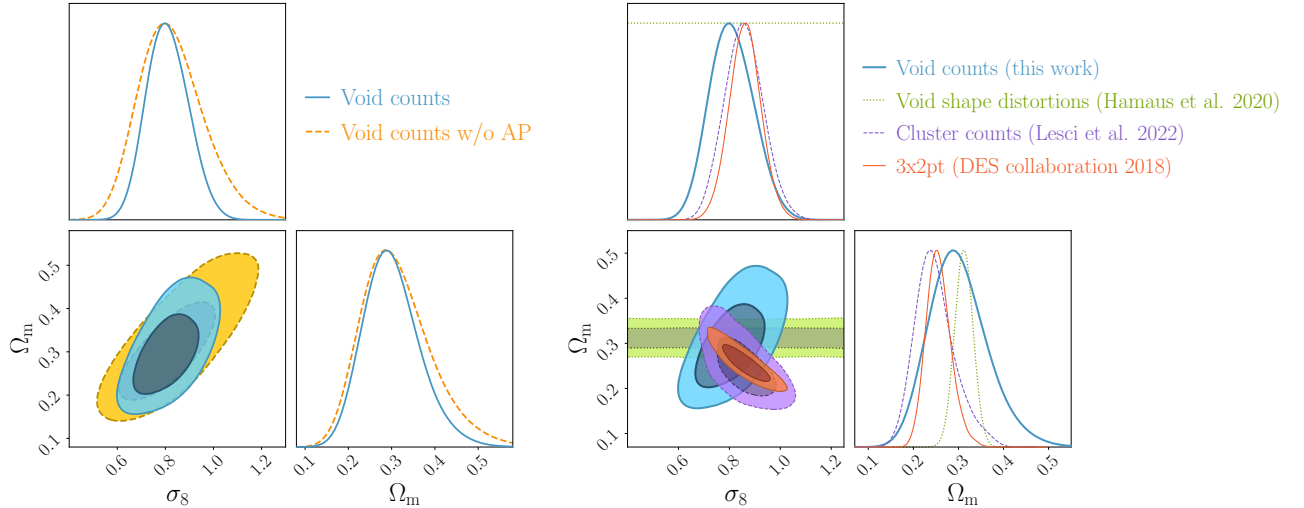


Figure 1. 68% and 95% confidence contours on the Ω_m - σ_8 parameter plane and the corresponding projected posterior distributions. *Left:* constraints from void counts (in light blue) compared to the confidence contours obtained without including the void radius correction for the AP effect (in orange, see Section 3). *Right:* comparison of the results from void counts with other cosmological probes: void shape distortions in green (Hamaus et al. 2020), cluster counts in purple (Lesci et al. 2022) and the DES Y1 3x2pt analysis in red (Dark Energy Survey Collaboration et al. 2018).

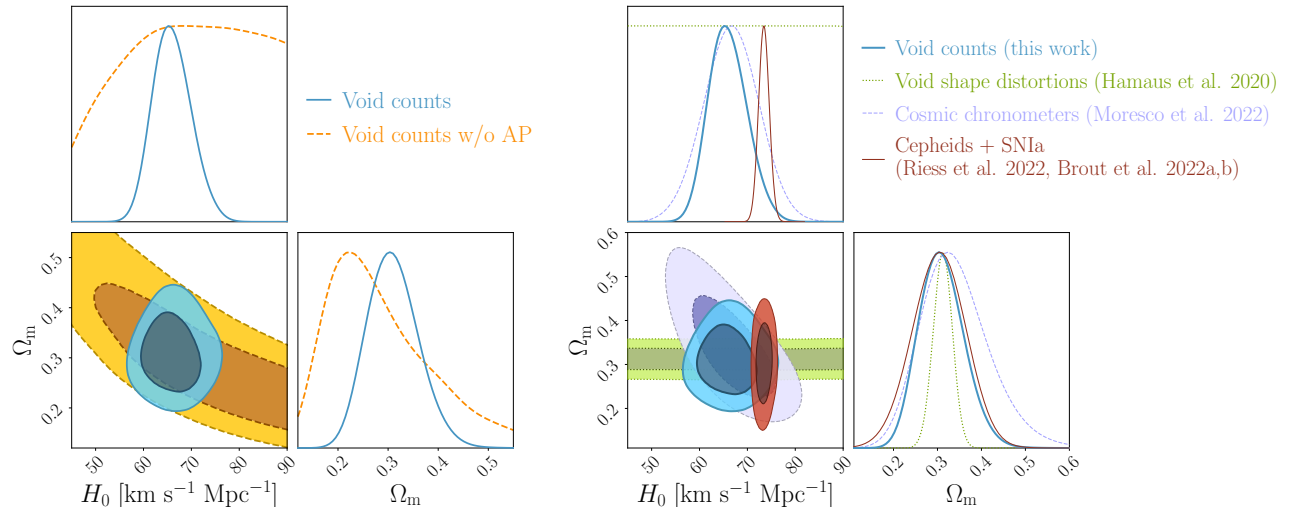


Figure 2. Same as Figure 1, but for the Ω_m - H_0 parameter plane. In the right panel we now include constraints from cosmic chronometers in violet (Moresco et al. 2022) and from the distance ladder in dark red (Cepheids+SNIa, Riess et al. 2022; Brout et al. 2022a,b).

tational lensing³ performed by the Dark Energy Survey Collaboration et al. (2018) with data from the first year of observations (DES Y1).

As expected from previous works (Bayer et al. 2021; Kreisch et al. 2022; Contarini et al. 2022a; Pellicciari et al. 2022), the constraints on Ω_m and σ_8 obtained from the analysis of the void size function are notably perpendic-

ular to those derived from standard probes. A brief explanation for the physical origin of this orthogonality is provided in Appendix C of Contarini et al. (2022b). We underline that this property is of key importance for the perspective of performing a joint cosmological analysis, especially considering that void counts are marginally correlated with statistics based on overdensities (see, e.g., Bayer et al. 2021; Kreisch et al. 2022).

In Figure 2 we present our results in the Ω_m - H_0 parameter plane. In this case we assume a void size function model with Ω_m and H_0 as free parameters (see Sec-

³ This analysis concerns the modeling of three two-point functions: the cosmic shear correlation function, the galaxy angular auto-correlation and the galaxy-shear cross-correlation, and is commonly abbreviated as 3x2pt.

tion 3) and obtain $\Omega_m = 0.303^{+0.053}_{-0.049}$ and $H_0 = 65.2^{+4.5}_{-3.6}$ km s⁻¹ Mpc⁻¹. In the left panels we show the effect of the AP correction on the cosmological constraints. It clearly emerges that, when geometric distortions are included in the modeling of void counts, the precision increases significantly, especially on the estimate of H_0 .

In the right panels of Figure 2 we compare these constraints with selected noteworthy results from the literature. As in Figure 1, we report the estimate of Ω_m from Hamaus et al. (2020), the constraints obtained by Moresco et al. (2022) via the study of cosmic chronometers extracted from a combination of spectroscopic surveys, and the publicly available⁴ results from the analysis of SN Ia, selected in the Pantheon+ sample (Scolnic et al. 2022; Brout et al. 2022a,b) including the cepheid host distances and covariance (SH0ES program, Riess et al. 2022). As described more in detail in Section 4.2, the latter derive a value of H_0 in slight disagreement with the constraints obtained in this work, as the two estimates are statistically incompatible at more than 1σ .

4.2. The void perspective on cosmological tensions

In this section we firstly compute the value of S_8 derived with the modeling of BOSS DR12 void counts and then compare it with selected results from the literature. Our analysis yields a value of $S_8 = 0.78^{+0.16}_{-0.14}$, which is constrained with a precision of about 19%. We note that this relatively large uncertainty is related to the definition of S_8 : this derived parameter follows the main degeneracy direction of weak lensing and cluster counts measurements, which is unfavourable for perpendicular constraints, such as those obtained in our analysis.

In Figure 3 we compare our result with the constraints derived in the following works (from top to bottom): Planck Collaboration et al. (2020) from CMB temperature and polarization, Semenaite et al. (2022) from the full shape of anisotropic clustering measurements in BOSS and eBOSS, Lesci et al. (2022) from the mass function of clusters in KiDS DR3, the Dark Energy Survey Collaboration et al. (2018) from the 3x2pt analysis in DES Y1, Asgari et al. (2021) from cosmic shear in KiDS-1000, Philcox & Ivanov (2022) from the large-scale galaxy power spectrum and bispectrum monopole in the BOSS DR12, and Heymans et al. (2021) from the 3x2pt analysis in KiDS-1000. Although our constraints cannot statistically exclude any of the S_8 estimates presented, we note that the precision on S_8 is expected to improve significantly when combining the results from void counts with standard cosmological probes thanks to the strong orthogonality between the corresponding Ω_m - σ_8

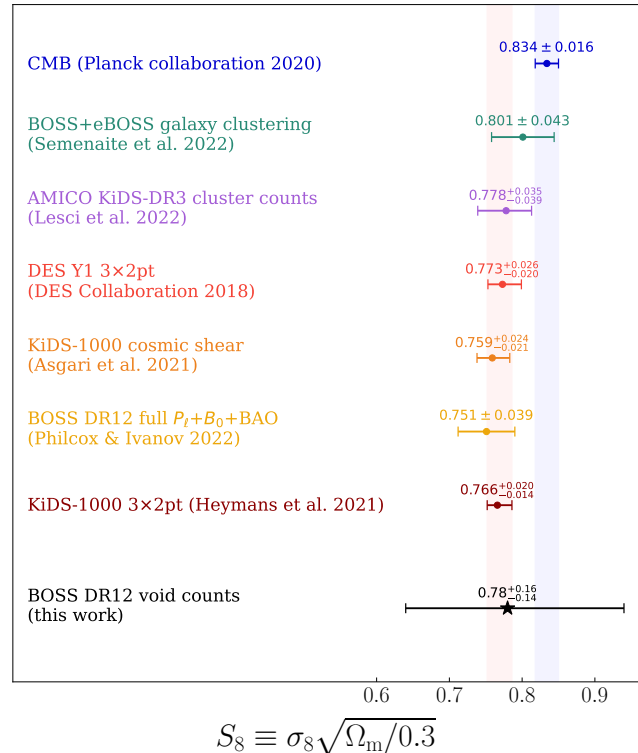


Figure 3. Comparison between recent constraints on the parameter S_8 from different cosmological probes, with error bars representing the 68% confidence intervals. From top to bottom: Planck Collaboration et al. (2020), Semenaite et al. (2022), Lesci et al. (2022), Dark Energy Survey Collaboration et al. (2018), Asgari et al. (2021), Philcox & Ivanov (2022) and Heymans et al. (2021). The first and the last of these trace two reference bands, in blue and red respectively, to highlight the disagreement between the results at high and low redshift. We report our constraint on S_8 on the bottom, with a black star with error bars.

confidence contours (see Section 4.1). This has indeed recently been highlighted by Pellicciari et al. (2022), who demonstrated that a joint analysis of cluster and void number counts can reduce the uncertainty on the S_8 parameter by approximately 40% compared to cluster counts taken as a stand-alone probe.

Moving on to the Hubble constant, in Figure 4 we present a comparison of our estimate ($H_0 = 65.2^{+4.5}_{-3.6}$ km s⁻¹ Mpc⁻¹) with recent selected cosmological constraints from the literature. Going from top to bottom we report the results by: the Planck Collaboration et al. (2020) from the analysis of CMB anisotropies, Moresco et al. (2022) from the study of cosmic chronometers, Semenaite et al. (2022) from the anisotropic clustering measurements in BOSS and eBOSS, The LIGO Scientific Collaboration et al. (2021) using gravitational-wave sources extracted from the third LIGO-Virgo-KAGRA (LVK) Gravitational-Wave

⁴ <https://github.com/PantheonPlusSH0ES/DataRelease>

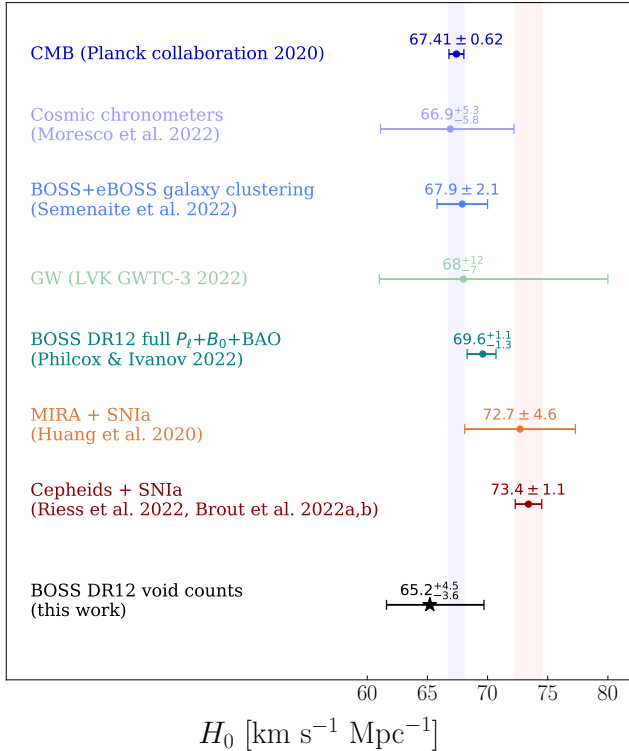


Figure 4. As Figure 3, but for the Hubble constant H_0 . Here we compare our constraints (in black) with: Planck Collaboration et al. (2020), Moresco et al. (2022), Semenaitte et al. (2022), The LIGO Scientific Collaboration et al. (2021), Philcox & Ivanov (2022), Huang et al. (2020) and Riess et al. (2022); Brout et al. (2022a,b).

Transient Catalog (GWTC-3), Philcox & Ivanov (2022) from the full shape analysis of the power spectrum and bispectrum monopole of BOSS DR12 galaxies, Huang et al. (2020) exploiting the luminosity of a SN Ia calibrated with Hubble Space Telescope Mira variables, and finally Riess et al. (2022) and Brout et al. (2022a,b) from the analysis of Pantheon+ SN Ia calibrated with cepheids. From this plot it is easy to appreciate how our estimate of H_0 is fully consistent with all the presented cosmological constraints, except for those obtained from Pantheon+ SN Ia calibrated with cepheids. However, considering broader error bars with 95% confidence levels also brings these into agreement. Therefore, our analysis favors a value of H_0 closer to the Planck Collaboration et al. (2020) results, but at this stage does not significantly disagree with the low-redshift constraints based on the SN Ia distance ladder method.

5. Conclusions

In this *Letter*, we analyzed the size function of voids identified in the BOSS DR12 galaxies (Reid et al. 2016). We computed the void number counts in two redshift

bins and modeled them by means of an extension of the popular Vdn model (Jennings et al. 2013; Contarini et al. 2019, 2022b). The latter relies on two nuisance parameters, C_{slope} and C_{offset} , that we calibrated using 100 realizations of the official BOSS MultiDark PATCHY simulations (Kitaura et al. 2016). The modeling that we considered consistently accounts for redshift-space and geometric distortions and was validated in Contarini et al. (2022b) on the PATCHY mocks. We focused on the Ω_m - σ_8 and Ω_m - H_0 parameter planes, comparing our results with other selected noteworthy cosmological constraints from the literature, in the light of the modern cosmological tensions.

First, we analyzed BOSS void counts to investigate the $S_8 \equiv \sigma_8 \sqrt{\Omega_m/0.3}$ tension. We previously obtained the marginalized constraints $\Omega_m = 0.286^{+0.070}_{-0.057}$ and $\sigma_8 = 0.797^{+0.094}_{-0.081}$, which translate into the derived parameter $S_8 = 0.78^{+0.16}_{-0.14}$. These results are compatible with cosmological constraints derived from other probes, such as the void-galaxy cross-correlation function, galaxy cluster number counts, the 3x2pt statistics and others. We underline that the confidence contours presented in this work are notably orthogonal to those derived from standard cosmological probes (as previously highlighted by Bayer et al. 2021; Kreisch et al. 2022; Contarini et al. 2022a; Pellicciari et al. 2022). This reveals the importance of combining void counts with different probes to tackle the S_8 tension.

We then oriented our analysis towards the H_0 tension, deriving the marginalized constraints $\Omega_m = 0.303^{+0.053}_{-0.049}$ and $H_0 = 65.2^{+4.5}_{-3.6}$ km s⁻¹ Mpc⁻¹. These are in agreement with various results from the literature, such as those derived from the analysis of CMB anisotropies in the Planck Collaboration et al. (2020), but are in mild disagreement with the constraints from SN Ia by Riess et al. (2022) and Brout et al. (2022a,b).

The constraints on the parameters S_8 and H_0 we presented are the first ever derived from cosmic voids and we plan to extend our analysis to the data of upcoming wide-field surveys like *Euclid* (Laureijs et al. 2011; Amendola et al. 2018), the Dark Energy Spectroscopic Instrument (DESI Collaboration et al. 2016), the Prime Focus Spectrograph (PFS, Tamura et al. 2016), the Nancy Grace Roman Space Telescope (NGRST, Spergel et al. 2015), the Spectro-Photometer for the History of the Universe and Ices Explorer (SPHEREx, Doré et al. 2018), and the Vera C. Rubin Observatory (Ivezić et al. 2019). In the near future we expect void counts to provide a fundamental contribution in shedding light on the rising tensions in cosmology, especially when included in a joint analysis with independent cosmological probes.

SC thanks Michele Moresco, Alfonso Veropalumbo, Giorgio Lesci and Nicola Borghi for the contribution and suggestions they provided. AP is grateful to Scott Dodelson for useful discussions. The authors thank Stefan Hagstotz, Barbara Sartoris, Nico Schuster, Giovanni Verza and Ben Wandelt for useful conversations. We acknowledge the grant ASI n.2018-23-HH.0. SC, FM, LM and MB acknowledge the use of computational resources from the parallel computing cluster of the Open Physics Hub (<https://site.unibo.it/openphysicshub/en>) at the Physics and Astronomy Department in Bologna. AP is supported by NASA ROSES grant 12-EUCLID12-0004, and NASA grant 15-WFIRST15-0008 to the Nancy Grace Roman Space Telescope Science Investigation Team “Cosmology with the High Latitude Survey”. AP acknowledges support from the Simons Foundation to the Center for Computational Astrophysics at the Flatiron Institute. NH is supported by the Excellence Cluster ORIGINS, which is funded by the Deutsche Forschungsgemeinschaft (DFG, German Research Foundation) under Germany’s Excellence Strategy – EXC-2094 – 390783311. LM acknowledges support from PRIN MIUR 2017 WSCC32 “Zooming into dark matter and proto-galaxies with massive lensing clusters”. We acknowledge use of the Python libraries NumPy (Harris et al. 2020), Matplotlib (Hunter 2007) and ChainConsumer (Hinton 2016).

References

- Abdalla, E., Abellán, G. F., Aboubrahim, A., et al. 2022, *Journal of High Energy Astrophysics*, 34, 49, doi: [10.1016/j.jheap.2022.04.002](https://doi.org/10.1016/j.jheap.2022.04.002)
- Alcock, C., & Paczynski, B. 1979, *Nature*, 281, 358, doi: [10.1038/281358a0](https://doi.org/10.1038/281358a0)
- Amendola, L., Appleby, S., Avgoustidis, A., et al. 2018, *Living Reviews in Relativity*, 21, 2, doi: [10.1007/s41114-017-0010-3](https://doi.org/10.1007/s41114-017-0010-3)
- Asgari, M., Lin, C.-A., Joachimi, B., et al. 2021, *A&A*, 645, A104, doi: [10.1051/0004-6361/202039070](https://doi.org/10.1051/0004-6361/202039070)
- Aubert, M., Cousinou, M.-C., Escoffier, S., et al. 2022, *MNRAS*, 513, 186, doi: [10.1093/mnras/stac828](https://doi.org/10.1093/mnras/stac828)
- Bayer, A. E., Villaescusa-Navarro, F., Massara, E., et al. 2021, *ApJ*, 919, 24, doi: [10.3847/1538-4357/ac0e91](https://doi.org/10.3847/1538-4357/ac0e91)
- Bayer, A. E., Liu, J., Terasawa, R., et al. 2022, arXiv e-prints, arXiv:2210.15647, <https://arxiv.org/abs/2210.15647>
- Bonici, M., Carbone, C., Vielzeuf, P., et al. 2022, arXiv e-prints, arXiv:2206.14211, <https://arxiv.org/abs/2206.14211>
- Brout, D., Taylor, G., Scolnic, D., et al. 2022a, *ApJ*, 938, 111, doi: [10.3847/1538-4357/ac8bcc](https://doi.org/10.3847/1538-4357/ac8bcc)
- Brout, D., Scolnic, D., Popovic, B., et al. 2022b, *ApJ*, 938, 110, doi: [10.3847/1538-4357/ac8e04](https://doi.org/10.3847/1538-4357/ac8e04)
- Contarini, S., Verza, G., Pisani, A., et al. 2022a, *A&A*, 667, A162, doi: [10.1051/0004-6361/202244095](https://doi.org/10.1051/0004-6361/202244095)
- Contarini, S., Marulli, F., Moscardini, L., et al. 2021, *MNRAS*, 504, 5021, doi: [10.1093/mnras/stab1112](https://doi.org/10.1093/mnras/stab1112)
- Contarini, S., Pisani, A., Hamaus, N., et al. 2022b, arXiv e-prints, arXiv:2212.03873, <https://arxiv.org/abs/2212.03873>
- Contarini, S., Ronconi, T., Marulli, F., et al. 2019, *MNRAS*, 488, 3526, doi: [10.1093/mnras/stz1989](https://doi.org/10.1093/mnras/stz1989)
- Dark Energy Survey Collaboration, Abbott, T. M. C., Abdalla, F. B., et al. 2018, *PhRvD*, 98, 043526, doi: [10.1103/PhysRevD.98.043526](https://doi.org/10.1103/PhysRevD.98.043526)
- Dawson, K. S., Schlegel, D. J., Ahn, C. P., et al. 2013, *AJ*, 145, 10, doi: [10.1088/0004-6256/145/1/10](https://doi.org/10.1088/0004-6256/145/1/10)
- DESI Collaboration, Aghamousa, A., Aguilar, J., et al. 2016, arXiv:1611.00036, <https://arxiv.org/abs/1611.00036>
- Di Valentino, E., Anchordoqui, L. A., Akarsu, Ö., et al. 2021a, *Astroparticle Physics*, 131, 102605, doi: [10.1016/j.astropartphys.2021.102605](https://doi.org/10.1016/j.astropartphys.2021.102605)
- . 2021b, *Astroparticle Physics*, 131, 102604, doi: [10.1016/j.astropartphys.2021.102604](https://doi.org/10.1016/j.astropartphys.2021.102604)
- Di Valentino, E., Mena, O., Pan, S., et al. 2021c, *Classical and Quantum Gravity*, 38, 153001, doi: [10.1088/1361-6382/ac086d](https://doi.org/10.1088/1361-6382/ac086d)
- Doré, O., Werner, M. W., Ashby, M. L. N., et al. 2018, arXiv:1805.05489, <https://arxiv.org/abs/1805.05489>
- Eisenstein, D. J., Weinberg, D. H., Agol, E., et al. 2011, *AJ*, 142, 72, doi: [10.1088/0004-6256/142/3/72](https://doi.org/10.1088/0004-6256/142/3/72)
- Hamaus, N., Aubert, M., Pisani, A., et al. 2022, *A&A*, 658, A20, doi: [10.1051/0004-6361/202142073](https://doi.org/10.1051/0004-6361/202142073)
- Hamaus, N., Pisani, A., Choi, J.-A., et al. 2020, *JCAP*, 2020, 023, doi: [10.1088/1475-7516/2020/12/023](https://doi.org/10.1088/1475-7516/2020/12/023)
- Hamaus, N., Pisani, A., Sutter, P. M., et al. 2016, *PhRvL*, 117, 091302, doi: [10.1103/PhysRevLett.117.091302](https://doi.org/10.1103/PhysRevLett.117.091302)
- Harris, C. R., Millman, K. J., van der Walt, S. J., et al. 2020, *Nature*, 585, 357, doi: [10.1038/s41586-020-2649-2](https://doi.org/10.1038/s41586-020-2649-2)
- Heymans, C., Tröster, T., Asgari, M., et al. 2021, *A&A*, 646, A140, doi: [10.1051/0004-6361/202039063](https://doi.org/10.1051/0004-6361/202039063)
- Hinton, S. R. 2016, *The Journal of Open Source Software*, 1, 00045, doi: [10.21105/joss.00045](https://doi.org/10.21105/joss.00045)
- Huang, C. D., Riess, A. G., Yuan, W., et al. 2020, *ApJ*, 889, 5, doi: [10.3847/1538-4357/ab5dbd](https://doi.org/10.3847/1538-4357/ab5dbd)
- Hunter, J. D. 2007, *Computing in Science & Engineering*, 9, 90, doi: [10.1109/MCSE.2007.55](https://doi.org/10.1109/MCSE.2007.55)
- Ivezić, Ž., Kahn, S. M., Tyson, J. A., et al. 2019, *ApJ*, 873, 111, doi: [10.3847/1538-4357/ab042c](https://doi.org/10.3847/1538-4357/ab042c)
- Jennings, E., Li, Y., & Hu, W. 2013, *MNRAS*, 434, 2167, doi: [10.1093/mnras/stt1169](https://doi.org/10.1093/mnras/stt1169)
- Kitaura, F.-S., Rodríguez-Torres, S., Chuang, C.-H., et al. 2016, *MNRAS*, 456, 4156, doi: [10.1093/mnras/stv2826](https://doi.org/10.1093/mnras/stv2826)
- Kitaura, F. S., Yepes, G., & Prada, F. 2014, *MNRAS*, 439, L21, doi: [10.1093/mnrasl/slt172](https://doi.org/10.1093/mnrasl/slt172)
- Klypin, A., Yepes, G., Gottlöber, S., Prada, F., & Heß, S. 2016, *MNRAS*, 457, 4340, doi: [10.1093/mnras/stw248](https://doi.org/10.1093/mnras/stw248)
- Kovács, A., Vielzeuf, P., Ferrero, I., et al. 2022, *MNRAS*, 515, 4417, doi: [10.1093/mnras/stac2011](https://doi.org/10.1093/mnras/stac2011)
- Kreisch, C. D., Pisani, A., Villaescusa-Navarro, F., et al. 2022, *ApJ*, 935, 100, doi: [10.3847/1538-4357/ac7d4b](https://doi.org/10.3847/1538-4357/ac7d4b)
- Laureijs, R., Amiaux, J., Arduini, S., et al. 2011, arXiv e-prints, <https://arxiv.org/abs/1110.3193>

- Lesci, G. F., Marulli, F., Moscardini, L., et al. 2022, *A&A*, 659, A88, doi: [10.1051/0004-6361/202040194](https://doi.org/10.1051/0004-6361/202040194)
- Marulli, F., Veropalumbo, A., & Moresco, M. 2016, *Astronomy and Computing*, 14, 35, doi: [10.1016/j.ascom.2016.01.005](https://doi.org/10.1016/j.ascom.2016.01.005)
- Moresco, M., Amati, L., Amendola, L., et al. 2022, arXiv:2201.07241. <https://arxiv.org/abs/2201.07241>
- Nadathur, S., Woodfinden, A., Percival, W. J., et al. 2020, *MNRAS*, 499, 4140, doi: [10.1093/mnras/staa3074](https://doi.org/10.1093/mnras/staa3074)
- Neyrinck, M. C. 2008, *MNRAS*, 386, 2101, doi: [10.1111/j.1365-2966.2008.13180.x](https://doi.org/10.1111/j.1365-2966.2008.13180.x)
- Pandey, K. L., Karwal, T., & Das, S. 2020, *JCAP*, 2020, 026, doi: [10.1088/1475-7516/2020/07/026](https://doi.org/10.1088/1475-7516/2020/07/026)
- Pellicciari, D., Contarini, S., Marulli, F., et al. 2022, arXiv e-prints, arXiv:2210.07248. <https://arxiv.org/abs/2210.07248>
- Philcox, O. H. E., & Ivanov, M. M. 2022, *PhRvD*, 105, 043517, doi: [10.1103/PhysRevD.105.043517](https://doi.org/10.1103/PhysRevD.105.043517)
- Pisani, A., Massara, E., Spergel, D. N., et al. 2019, *BAAS*, 51, 40. <https://arxiv.org/abs/1903.05161>
- Planck Collaboration, Ade, P. A. R., Aghanim, N., et al. 2014, *A&A*, 571, A16, doi: [10.1051/0004-6361/201321591](https://doi.org/10.1051/0004-6361/201321591)
- Planck Collaboration, Aghanim, N., Akrami, Y., et al. 2020, *A&A*, 641, A1, doi: [10.1051/0004-6361/201833880](https://doi.org/10.1051/0004-6361/201833880)
- Platen, E., van de Weygaert, R., & Jones, B. J. T. 2007, *MNRAS*, 380, 551, doi: [10.1111/j.1365-2966.2007.12125.x](https://doi.org/10.1111/j.1365-2966.2007.12125.x)
- Reid, B., Ho, S., Padmanabhan, N., et al. 2016, *MNRAS*, 455, 1553, doi: [10.1093/mnras/stv2382](https://doi.org/10.1093/mnras/stv2382)
- Riess, A. G., Yuan, W., Macri, L. M., et al. 2022, *ApJL*, 934, L7, doi: [10.3847/2041-8213/ac5c5b](https://doi.org/10.3847/2041-8213/ac5c5b)
- Rodríguez-Torres, S. A., Chuang, C.-H., Prada, F., et al. 2016, *MNRAS*, 460, 1173, doi: [10.1093/mnras/stw1014](https://doi.org/10.1093/mnras/stw1014)
- Ronconi, T., Contarini, S., Marulli, F., Baldi, M., & Moscardini, L. 2019, *MNRAS*, 488, 5075, doi: [10.1093/mnras/stz2115](https://doi.org/10.1093/mnras/stz2115)
- Ronconi, T., & Marulli, F. 2017, *A&A*, 607, A24, doi: [10.1051/0004-6361/201730852](https://doi.org/10.1051/0004-6361/201730852)
- Sahlén, M., Zubeldía, Í., & Silk, J. 2016, *ApJL*, 820, L7, doi: [10.3847/2041-8205/820/1/L7](https://doi.org/10.3847/2041-8205/820/1/L7)
- Sánchez, A. G., Scoccimarro, R., Crocce, M., et al. 2017, *MNRAS*, 464, 1640, doi: [10.1093/mnras/stw2443](https://doi.org/10.1093/mnras/stw2443)
- Schöneberg, N., Abellán, G. F., Sánchez, A. P., et al. 2022, *PhR*, 984, 1, doi: [10.1016/j.physrep.2022.07.001](https://doi.org/10.1016/j.physrep.2022.07.001)
- Scolnic, D., Brout, D., Carr, A., et al. 2022, *ApJ*, 938, 113, doi: [10.3847/1538-4357/ac8b7a](https://doi.org/10.3847/1538-4357/ac8b7a)
- Semenaite, A., Sánchez, A. G., Pezzotta, A., et al. 2022, *MNRAS*, 512, 5657, doi: [10.1093/mnras/stac829](https://doi.org/10.1093/mnras/stac829)
- Sheth, R. K., & van de Weygaert, R. 2004, *MNRAS*, 350, 517, doi: [10.1111/j.1365-2966.2004.07661.x](https://doi.org/10.1111/j.1365-2966.2004.07661.x)
- Spergel, D., Gehrels, N., Baltay, C., et al. 2015, arXiv:1503.03757. <https://arxiv.org/abs/1503.03757>
- Sutter, P. M., Lavaux, G., Hamaus, N., et al. 2015, *Astronomy and Computing*, 9, 1, doi: [10.1016/j.ascom.2014.10.002](https://doi.org/10.1016/j.ascom.2014.10.002)
- Tamura, N., Takato, N., Shimono, A., et al. 2016, in *Society of Photo-Optical Instrumentation Engineers (SPIE) Conference Series*, Vol. 9908, Ground-based and Airborne Instrumentation for Astronomy VI, ed. C. J. Evans, L. Simard, & H. Takami, 99081M, doi: [10.1117/12.2232103](https://doi.org/10.1117/12.2232103)
- Taruya, A., Nishimichi, T., & Saito, S. 2010, *PhRvD*, 82, 063522, doi: [10.1103/PhysRevD.82.063522](https://doi.org/10.1103/PhysRevD.82.063522)
- The LIGO Scientific Collaboration, the Virgo Collaboration, the KAGRA Collaboration, et al. 2021, arXiv e-prints, arXiv:2111.03604. <https://arxiv.org/abs/2111.03604>
- Verza, G., Pisani, A., Carbone, C., Hamaus, N., & Guzzo, L. 2019, *JCAP*, 2019, 040, doi: [10.1088/1475-7516/2019/12/040](https://doi.org/10.1088/1475-7516/2019/12/040)
- Woodfinden, A., Nadathur, S., Percival, W. J., et al. 2022, *MNRAS*, 516, 4307, doi: [10.1093/mnras/stac2475](https://doi.org/10.1093/mnras/stac2475)